

# Quantum buses and quantum computer architecture based on quantum dots

Irene D'Amico\*

Department of Physics, University of York, York YO10, United Kingdom

(Dated: June 25, 2018)

We propose a quantum computer architecture based on quantum dots both for short distance and for long distance communication/computation. Our scheme exploits the natural characteristics of self-assembled quantum dots and it is scalable. It is centered on the idea of a quantum bus based on semiconductor self-assembled quantum dots. This allows for transmission of qubits between the different quantum registers, and could be integrated in most of the present proposal for semiconductor quantum dot-based quantum computation. Our proposal exploits the peculiar properties of *relatively short* spin-chains, and advantages and disadvantages of two possible implementations, both based on spin-chain global dynamics, are discussed in details. A clear advantage of the scheme is to avoid the use of microcavities for long distance communication between different elements of the quantum computer. In this respect our scheme is comparatively faster than hybrid quantum dot-microcavity schemes.

PACS numbers: 03.67.Lx, 78.67.Hc, 85.35.-p, 03.67.-a

## I. INTRODUCTION

In the past years, self-assembled semiconductor quantum dots<sup>1</sup> have been considered one of the most promising hardware for envisaging quantum information/computation (QIC) schemes (see e.g. Ref. 2,3,4,5,6,7,8). The key feature of this hardware is the possibility of optically drive quantum calculations by multicolor trains of laser pulses, overcoming in this way the relatively fast decoherence times typical of solid state systems. Another important characteristic is the fact that, since self-assembled quantum dots (QDs) tend to be naturally produced in large arrays, such a hardware could in principle solve the problem of scalability, which affects other types of implementations.

Many QD-based QIC schemes consider as quantum arrays ensembles of vertically stacked quantum dots<sup>2,3,4,6,7</sup>, which spontaneously form in multilayer QD structures<sup>1</sup>. However following the initial enthusiasm, it has become clear that this choice solves only partially the scalability problem. Experiments show in fact that the maximum length of such vertical arrays is of the order of ten quantum dots only. Clearly this rises the problem of how to perform complex computations or equivalently, how to communicate between different arrays. A possible solution for communicating between far away quantum dots/arrays is to embed the system in a microcavity and then to use the cavity mode to transmit qubits of information between well separated quantum dots. This exploits the potential conversion of trapped excitons into flying qubits and vice-versa<sup>5,8</sup>. Among the problematic issues related to this scheme are (i) to experimentally embed self-assembled arrays of quantum dot in a high Q microcavity, (ii) to carefully position the dots away from the cavity mode nodes in order to preserve QD-cavity coupling, (iii) to engineer the structure such that it is still possible to address the QDs by laser fields and possibly couple each QD with a static external electric fields, as required, e.g., in Ref. 2,3,7. Experimentally this is very demanding.

To lift these complex requirements, we propose to communicate between far away vertical arrays of QDs by using quantum buses made by *in-plane* chains of quantum dots. To im-

plement this, our proposal exploits the structural differences and peculiar characteristics of in-plane versus vertical arrays of self-assembled QDs.

The first part of the paper describes a possible global architecture for QD-based quantum computers. In the second part we will analyze different possibilities for implementing information transfer along the QD-based bus, which exploit the global dynamics of the system. We shall devolve particular attention to the constraints imposed on the scheme by the *physical* nature of the system itself. Later we shall discuss the robustness of the proposed schemes and compare the performances of our quantum bus against the use of a microcavity.

## II. QUANTUM COMPUTER HARDWARE DESIGN

Self-assembled quantum dots are characterized by different properties, depending if we are considering an ensemble of *in-plane* QDs (the plane being orthogonal to the direction of growth) or an array of QDs stacked in the growth direction. In the following we will refer to the latter structure as 'Vertically Stacked Array' (VSA).

VSAs have very distinctive characteristics. First of all they tend to form naturally due to strain propagation<sup>1</sup>. Secondly self-assembled quantum dots are strongly confined in the growth direction, due to bandgap mismatch between the different semiconductors. This implies that (i) particle tunneling between nearby, vertically stacked QDs can be more difficult, even for small QD-QD distances<sup>9</sup> (ii) QDs can be very close together and (iii) interactions between vertically coupled quantum dots may be quite strong (see e.g. Ref.2). The latter characteristic is very promising since quantum operations based on these interactions can be carried out in times much shorter than the relevant decoherence times<sup>2</sup>. Last but not least, due to the strain propagation, vertically stacked QDs tend to be noticeably different in size, which make them good candidates for energy selective addressing of specific excitations, a key ingredient in many QDs-based QIC proposals<sup>2,3,7</sup>.

On the other side in-plane quantum dots can be produced in fairly uniform size by controlling the growth parameters: at

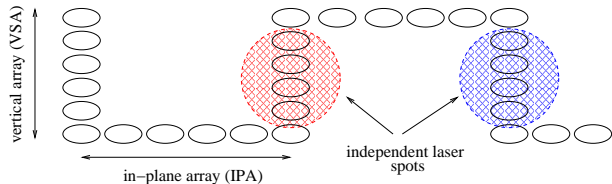


FIG. 1: Schematic sequence of vertical arrays (VSA) and in-plane arrays (IPA) of QDs. Different VSAs can be addressed by different laser spots.

present samples can be already mono-disperse up to only few percent size variation. This uniformity will be most probably improved much further in the near future, especially since another important technological application, such as QD-based lasing, requires monodispersity<sup>10</sup>. In addition there is already a good control of the in-plane QD density (which can be varied between  $10^9$  to  $10^{12}$   $\text{cm}^{-2}$ ) and, at the moment, techniques, e.g. 'seeding', to produce more regular in-plane distributions are proposed and tested<sup>11</sup>.

The differences outlined above, between VSA and in-plane QDs, suggest us to diversify the use of the two categories, when thinking to the hardware structure of a quantum computer. The structure we envisage in this paper is composed by a series of VSAs - for example laying in the same plane - connected by chains of in-plane QDs, which we will refer to as In-Plane Arrays (IPAs, see Fig. 1).

This design allows for compact implementation of a quantum computer, since in principle it may confine the hardware in a single slab. This architecture satisfies the request of easier lateral access (e.g. for wiring) and manipulation of each QD forming the computer (e.g. for applying external fields to specific dots). This design is also *scalable*, in the sense that the same basic structure (VSA plus related IPA) could be repeated at will, as well as the slab structure as a whole.

We underline that the hardware structure we propose has yet another very advantageous feature. It can be built such that (i) each quantum register (i.e. any VSA) would be addressable by energy selective schemes (exploiting the natural diversity of stacked QDs), as required by many QIC schemes<sup>2,3,7</sup>, but, at the same time, (ii) different quantum registers (different VSAs) could be also discriminated *spatially*, e.g by near-field techniques. This can be achieved by making the quantum buses (i.e. the IPAs), longer or of the order of  $1000\text{\AA}$  (see Fig. 1). In this way the different VSA can be spatially resolved by different laser pulses. This is a big improvement in respect to architectures which use energy selective addressing only: in our proposal even if the same laser color would in principle couple to one QD per VSA, we would be still able to address these resonant quantum dots *separately*. In general we could identify the QD sequence in each VSA with a *short*, well defined laser color sequence, and this sequence could then be repeated (totally or partially) for different VSA. In principle the whole hardware structure could be built as a stacked sequence of mono-disperse QD planes, subsequently e.g. etched to form the VSA-IPA chosen structure. This combined spatial-plus-

energy selective addressability strongly enhances the hardware flexibility and helps overcoming the problems related to schemes which use energy-selective addressing only (e.g. NMR-based schemes).

### III. QUANTUM-DOT QUANTUM-BUS POTENTIAL IMPLEMENTATIONS

VSAs have been analyzed in details in many QIC proposals<sup>2,3,7</sup>; in this paper we will concentrate on possible ways of implementing a quantum-bus by using an IPA as hardware.

We will discuss in details two potential implementations which exploit the *global dynamics* of excitons in the IPAs. In both cases we shall (i) consider that state-of-the-art in-plane QDs can be made mono-disperse up to few percents and (ii) discuss a way to fine-tune QD-QD interactions *a posteriori*.

#### A. Implementation by global dynamics: general considerations

Recently there have been interesting developments in the study of the global dynamics of a spin-chain<sup>12,13,14,15</sup> as a possible way of transferring quantum information across the chain. It is well known that the time necessary to transfer information along a spin or pseudo-spin chain in QIC schemes based on nearest-neighbor gating operations (e.g. see Ref. 2,3,4,7) scales with the number of spins. There is though a widespread feeling that, when the transfer of information along a spin chain is based on the chain global dynamics, the transferring time can be independent from the chain length.

We will explicitly show that, for real systems, the time  $t_t$  for transferring a qubit of information across a spin chain still depends on the chain length (for our specific hardware the number of QDs forming the IPA). In some cases though and for the same chain length,  $t_t$  may be smaller when exploiting global dynamics than by using nearest-neighbor gating operations, and some other advantages may occur in the first case.

To understand why this is so, we must take into consideration some very general constraints, which are due to the fact that any hardware systems is indeed a physical system. These constraints are often overlooked in more abstract descriptions of spin-chain global dynamics; when 'translating' the schemes into a physical system though, physical limitations must be taken into consideration.

Let us consider a spin-chain global dynamics based on nearest-neighbor interactions  $J_{i,i+1}$ 's which are *modulated* along the chain,

$$J_{i,i+1} = J \cdot f(N), \quad (1)$$

where  $J$  is a constant representing a typical energy scale of the system and  $f(N)$  is the function describing the coupling modulation along the chain. We assume the modulation to be a reasonably regular function and to be un-bounded, so that  $f$  will depend over the chain length  $N$ .

The physical constraints in applying this scheme to any concrete system are connected to the following observations: (i) in any physical system there will be an upper limit  $J_{max}$  to the interaction strength, i.e.

$$\max\{J_{i,i+1}\} \leq J_{max} \quad (2)$$

and (ii) for practical purposes the transfer time  $t_t$  must be smaller than the typical decoherence times, i.e.

$$t_t < \tau_{dec}. \quad (3)$$

We shall show that Eqs. (2) and (3) (i) imply that the transfer time  $t_t$  across the chain depends over the chain length  $N$  and that (ii) this sets a physical limitation to the maximum length of the chain we can consider.

From Eq. (2) and Eq. (1) we have

$$J \cdot f(N) \leq J_{max}. \quad (4)$$

Since  $J/\hbar$  is the typical frequency of the system, we can assume that  $t_t \sim (J/\hbar)^{-1}$ . From Eq. (4) we obtain

$$\frac{f(N)}{J_{max}} \leq t_t, \quad (5)$$

which shows that (i) the transferring time has a lower bound and, more important, (ii) this lower bound (and hence the transferring time) depends on the chain length  $N$ . Using now Eq. (3), we obtain

$$\frac{f(N)}{J_{max}} < \tau_{dec}, \quad (6)$$

which sets a *physical* upper limit to the mathematically unbounded  $f(N)$  and hence to the chain length  $N$ .

For chains in which the modulation of the couplings  $\{J_i\}$  is bounded, the dependence of  $t_t$  on the chain length  $N$  is due at least to the constraint that information cannot travel faster than light. This is clearly a much weaker constraint, and, as we shall see below, our calculations show that, even for the extreme case of chains with un-modulated couplings, much stringent relations between  $t_t$  and  $N$  usually occur.

Among the various proposals related to spin chain global dynamics, we will first consider the one described in Ref. 12. This is a scheme for perfect transfer of information (a quantum state or two entangled states) across a spin chain, by exploiting the global time evolution of the system.

The requirement for perfect transfer is that the system is governed by a XY Hamiltonian, in which the non-diagonal couplings between nearby spins  $J_{i,i+1}$  must satisfy certain sequences, e.g.<sup>12</sup>

$$J_{i,i+1} = J\sqrt{i(N-i)}, \quad (7)$$

where  $N$  is number of spins in the chain and  $i = 1, \dots, N-1$ . Eq. (7) represents an unbounded modulation of the coupling strengths of the type considered in Eq. (1), which is in addition symmetric in respect to the centre of the spin chain. The time requested for the perfect transfer is<sup>12</sup>

$$t_{(n+1)pk} = (2n+1)\frac{\hbar\pi}{4J}, \quad (8)$$

$n = 0, 1, 2, \dots$ , and it is determined by the value of  $J$ .

In particular let us consider the transfer time corresponding to  $n = 0$ ,  $t_{1pk} = \hbar\pi/(4J)$  and rewrite Eq. (7) as

$$J = J_{max}/\sqrt{\text{int}(N/2) \cdot [N - \text{int}(N/2)]}, \quad (9)$$

where we have optimistically assumed that at the center of the chain  $J_{i,i+1} = J_{max}$ . Notice that the latter equation implies that

$$t_{1pk} \sim \frac{N}{2} \frac{\hbar}{J_{max}}, \quad (10)$$

i.e. there is direct proportionality between minimum time of transfer and chain length  $N$ . If we consider a transfer across a qubit chain done by nearest-neighbor two-qubit gates, and the ideal situation in which all the physical couplings used in the gates are given by  $J_{max}$ , we would have

$$t_{1pk} \sim N \frac{\hbar}{J_{max}}. \quad (11)$$

Comparing the last two equations, we see that the actual gain in using the global dynamics of a spin chain, when the *physical condition* of including a maximum strength for a coupling is taken into account, is a factor 2, coming from the symmetry of the modulation, but the transfer time still scales with the total number of spins  $N$ . Fig. 3, lower panel, shows  $t_{1pk}$  extracted from the simulation of spin chains with nearest-neighbor couplings following Eq. (7) in respect to  $N$ . It confirms the direct proportionality between minimum transfer time and chain length.

The concrete advantage of using global dynamics over two-qubit gating becomes then the possibility of simplifying the implementation, an issue that should not be underestimated, but may again depend over the specific physical characteristics of the system chosen as hardware. At the very least, exploiting global dynamics lifts the necessity of driving every single two qubit operation and this consequently avoids potential sources of errors; but what is really important when considering a spin chain global dynamics as a way to implement a quantum bus, is to maximize the simplicity of the device.

The fact that, as shown above, for physical realizations,  $N$  cannot be arbitrarily long, implies that the properties relevant to many practical implementations will be the ones of medium or relatively short chains, while previous literature has mainly focused on the large- $N$  limit<sup>13,15</sup>.

With this in mind, in the following we shall focus on chains characterized by  $N \lesssim 10$ , both underlining some specific general properties and referring to a specific physical system – the IPA-chain formed by QDs with excitons as pseudo-spins.

## B. Förster effect

We will consider implementations of quantum buses in which the coupling between nearby in-plane QDs is provided by the Förster effect<sup>16,17</sup>. Due to this coupling, the excitation corresponding to a correlated electron-hole pair (exciton) can be transferred from one QD to its neighbor.

This effect has been observed as a powerful motor for exciton transfer in colloidal self-assembled quantum dots<sup>17</sup>. The measured strength of the Förster coupling in CdSe QDs is of about 0.3 meV, but it is believed that in structurally optimized systems the interdot energy transfer can approach picosecond time scales, i.e. meV coupling strength<sup>17</sup>. Being the structures of interest to this paper (self-assembled QD) of similar size in respect to colloidal QD and being typical values for QD-QD interactions of few meV<sup>2</sup>, we will assume in our calculations 1 meV as a reasonable *upper limit* for Förster interaction in self-assembled QDs.

In the envelop function approximation, the Förster coupling between an exciton in QD<sub>i</sub> and an exciton in QD<sub>j</sub>,  $V_{Fij}$ , is given by<sup>18</sup>

$$V_{Fij} = \frac{O_i O_j e^2}{\epsilon R_{ij}^3} [\langle \mathbf{r}_i \rangle \langle \mathbf{r}_j \rangle - \frac{3}{R_{ij}^2} (\langle \mathbf{r}_i \rangle \cdot \mathbf{R}_{ij}) (\langle \mathbf{r}_j \rangle \cdot \mathbf{R}_{ij})] \quad (12)$$

where

$$O_i = \int \psi_e^i(\mathbf{r}) \psi_h^i(\mathbf{r}) d^3 r \quad (13)$$

is the overlap between the hole and electron envelop functions in QD<sub>i</sub>,  $R_{i,j}$  is the distance between QD<sub>i</sub> and QD<sub>j</sub>, and  $e \langle \mathbf{r}_i \rangle$  is the dipole moment due to the atomic part of the wave function in QD<sub>i</sub>.

We underline that no particle tunneling is involved in the Förster process, but only energy transfer: it depends in fact on  $O_i$ , the overlap of electron and hole wave-functions in the *same* QD. In tunneling, the relevant quantity is instead the overlap of wave-functions belonging to different QDs. Due to energy conservation, this coupling is most effective between very similar QDs. When QD chains are involved though, we can picture a dynamical Förster-based process between far-away but similar QDs positioned along the chain. The similarity of the first and last QD in the chain ensures that the total process of transferring the excitation across the IPA remains energy preserving.

Labeling with  $|0\rangle_i$  ( $|1\rangle_i$ ) the absence (the presence) of a single ground-state exciton in QD<sub>i</sub>, the Hamiltonian for a chain of  $N$  QDs, in which we consider at most single exciton occupancy of the IPA, is given by

$$H = \sum_i^N E_i |1\rangle_i \langle 1|_i + \sum_{i=1}^{N-1} (V_{Fij} |1\rangle_i \langle 0|_i \otimes |0\rangle_{i+1} \langle 1|_{i+1} + h.c.), \quad (14)$$

where we have assumed no single particle tunneling. Contributions behind nearest-neighbors are second order, since the Förster effect scale as  $R_{ij}^3$ , and have been neglected.

### C. Implementation by global dynamics using a QD chain: first method (modulated coupling)

For concreteness, in the following we shall consider as chain an IPA, and as (pseudo) spins degrees of freedom the presence or absence of a ground state exciton in each QD<sup>2</sup>. The transfer of quantum information across the ‘‘spin chain’’, will then correspond to the transfer of an excitonic state across the IPA, by means of exploiting the global excitonic dynamics of the system. The general conclusions on the IPA can though be easily transferred to other types of physical hardware.

The method we are going to discuss in details represents one of the possible schemes for transferring information between separate VSAs in the computer architecture previously outlined. To be able to address different VSAs with independent laser pulses, we require the length of the IPA to be longer than 1000Å. A reasonable distance between the center of nearby QDs is at least of the order of 150 – 200Å. This implies that the IPA must be formed by at least 5-7 QDs. The question is now if excitonic transfer through such a chain can be performed in a reasonable time and with reasonable accuracy.

In our system the (pseudo) spin degrees of freedom are represented by the presence ( $|1\rangle_i$ ) or absence ( $|0\rangle_i$ ) of a ground state exciton in each QD<sub>i</sub>, where  $i = 1, N$  labels sequentially the QDs in the chain. This is the same encoding proposed in Ref. 2. The Hamiltonian of the system is given by Eq. (14).

We shall refer to the scheme presented in Ref. 12 as the Modulated Coupling (MC) scheme. In respect to the XY Hamiltonian required by Ref. 12, Eq. (14) presents diagonal, in general not-equal, terms  $E_i$  and XY non-diagonal terms, provided by the Förster coupling  $V_{Fij}$ , which in general do not satisfy Eq. (7). To obtain a good approximation to the ‘mathematical’ Hamiltonian, we need at least to engineer the non-diagonal terms into the required sequence Eq. (7). From Eq. (12), we see that we can tune the value of the Förster coupling by (i) engineering the value of the interdot distance  $R_{ij}$  or (ii) by tuning the value of the overlap integrals  $O_i$ . Since roughly  $V_{Fij} \sim 1/R_{ij}^3$ , to engineer  $V_{Fij}$  according to Eq. (7) over an IPA of 5-7 QDs with  $R_i \sim 150 - 200\text{Å}$ , implies to be able to experimentally control  $R_{ij}$  up to few Amstrongs, which is at the moment experimentally very challenging. A more flexible approach, is to vary, *a posteriori*, the electron-hole function overlap  $O_i$ . This is doable by applying a suitable (but static) *in-plane* electric field to each QD, as described in Ref. 2. The field is to be applied in the in-plane direction orthogonal to the IPA’s direction (see Fig. 2). The advantage of this scheme is to allow also for corrections of possible errors occurred in the growth process, since the applied electric field can be varied *a posteriori*, after the growth process is completed.

Let us consider a ‘uniform’ initial condition, in which  $V_{Fi,i+1} = V_{Fj,j+1}$  for every  $i, j$ . If  $N = 5 - 7$  and  $\{V_{Fi,i+1}\}$  has to satisfy Eq. (7), the maximum correction required over the coupling strength  $V_{Fij}$  is of about 30%. This corresponds to a 20% variation over the overlap integrals  $O_i$ ’s. We need now to estimate the required electric field, in order to asses the feasibility of the scheme. If we assume Gaussian electron and

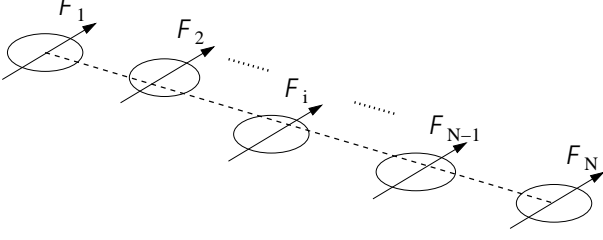


FIG. 2: Sketch of an IPA in which an external static electric field  $\mathcal{F}_i$  has been applied to every QD $_i$ .

hole wave-functions, the relation between  $O_i$  and the distance  $d$  between the wave-function centers is

$$O_i(d_i) = 2^{\frac{3}{2}} \prod_{t=x,y,z} \left[ \sqrt{\frac{\lambda_{te}\lambda_{th}}{\lambda_{te}^2 + \lambda_{th}^2}} \right]_i \exp\left(-\frac{1}{2} \frac{d_i^2}{\lambda_{xe,i}^2 + \lambda_{xh,i}^2}\right), \quad (15)$$

where  $\lambda_{t(e/h)}$  are the characteristic length of the wave-functions in the  $t = x, y, z$  directions. If we assume similar dots (a reasonable request for an IPA), we obtain

$$d_i \approx \sqrt{2(\lambda_{xe}^2 + \lambda_{xh}^2) \left| \ln\left(\frac{O_i}{O_{np}}\right) \right|}, \quad (16)$$

where  $O_{np}$ , is the unperturbed value of the overlap integral, i.e. the value it assumes for the central(s) QD(s) which is coupled to the neighbors by the coupling constant with the highest value (see Eq. (7)). On the other side  $d_i$  can be also related to the static electric field  $\mathcal{F}_i$  applied to QD $_i$  by<sup>2</sup>

$$d_i = e\mathcal{F}_i \left[ \frac{1}{m_e \omega_{e,i}^2} + \frac{1}{m_h \omega_{h,i}^2} \right]. \quad (17)$$

Assuming typical GaAs parameters ( $m_h = 0.34m_0$ ,  $m_e = 0.067m_0$ ,  $\hbar\omega_h \sim 20$  meV,  $\hbar\omega_e \sim 40$  meV), and using Eqs. (16) and (17), we see that a variation of 20% over the overlap integral  $O_i$  can be produced by a field of the order of 30KeV/cm, perfectly reasonable from the experimental point of view. We can then assert that the scheme we are going to describe more in details could in principle be implemented by state of the art technology.

#### D. Modulated coupling: simulations and errors

In this section we shall discuss and simulate the excitonic dynamics in IPAs and discuss the effect of possible sources of errors for the transmission of the excitonic state across the IPA. Because of the generality of most of the results, we will indicate the couplings as  $J_{i,i+1}$ , keeping in mind that when the considered hardware is an IPA the coupling is given by the Förster effect Eq. (12). We will consider in our calculations realistic QDs parameters and in particular GaAs-based IPAs with  $N \leq 9$  and  $J_{max} \leq 2$ meV,  $J_{max}$  the *upper limit* for the coupling between nearby QDs.

Let us first of all consider the case in which the conditions in Ref. 12 are perfectly satisfied. Fig. 3 (upper panel)

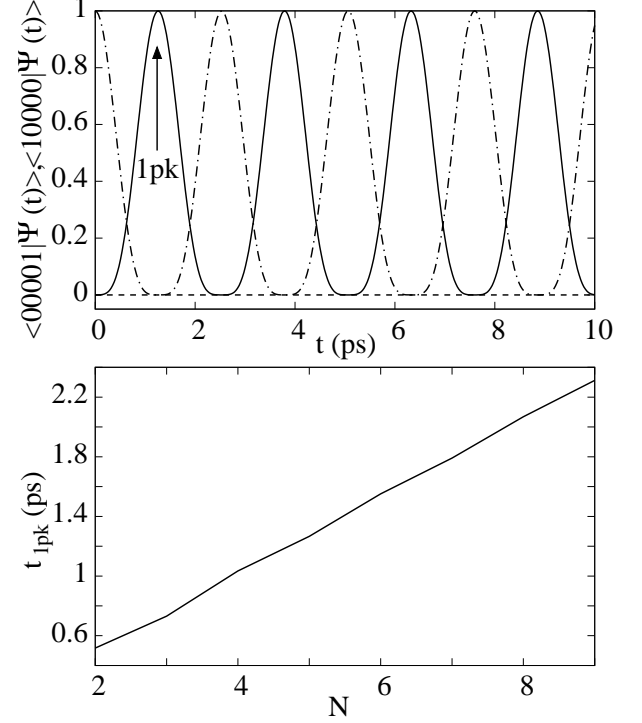


FIG. 3: Upper panel:  $\langle 10000|\Psi(t)\rangle$  (dashed-dot line) and  $\langle 00001|\Psi(t)\rangle$  (solid line) vs time for  $N=5$ . '1pk' marks the first resonance position. Lower panel:  $t_{1pk}$  vs  $N$ .

shows a simulation of the dynamics of the system for  $J_{max} = 1$ meV and an IPA of 5 QDs. The state at time  $t = 0$  is  $|\psi(0)\rangle = |10000\rangle$ , i.e. single exciton in QD $_1$ . The projection of the state of the system  $|\psi(t)\rangle$  at time  $t$  on the initial and the desired final state (i.e. exciton in QD $_N$ , the last QD),  $\langle 10\dots 0|\psi(t)\rangle$  and  $\langle 0\dots 01|\psi(t)\rangle$  respectively, are plotted. As predicted in Ref. 12, there is periodic perfect transfer between the two states, the first transfer occurring at  $t_{1pk} \approx 1.3$ ps. The lower panel presents the plot of the numerical value obtained for  $t_{1pk}$  when the length of the IPA is changed. As can be seen, the linear dependence of Eq. (10) is recovered. Notice that, even for  $N = 9$ , the transferring time remains very short,  $t_{1pk} \approx 2.3$ ps, confirming that, even if there is direct proportionality between  $N$  and  $t_{1pk}$ , at least for relatively short chains, the effect of this proportionality is not dramatic.

Let us compare these results with the use of microcavities, which is the alternative route for transferring information at 'long distance' in QD-based quantum computers. If we consider a *comparable* transfer done by mean of a microcavity, i.e. with a coupling of 1 meV between QDs and cavity, the minimum time necessary for the transfer is greater than 100 ps<sup>5</sup>. Extrapolating from Fig. 3, lower panel, and assuming the relation Eq. (10), a transferring time  $t_{1pk} = 100$ ps would correspond to a transfer over an IPA with  $N \approx 400$ , i.e., assuming  $R_{ij} = 150 \div 200 \text{ \AA}$ , over a distance of  $6 \div 8 \mu m$ . We see than that, from the transfer-time point of view, the use of microcavities becomes advantageous only when really long

distances, of the order of several microns, are involved. For these distances the design and modulation of long spin-chains (long IPAs) may also become too complicated.

We notice also that a phase shift is originated at the end of the transfer, depending on the number of QDs  $N^{12}$ . In particular when  $N - 1$  is an exact multiple of 4, no phase shift is produced<sup>12</sup>. Since, once the length of the chain is known, this fixed shift can be corrected by a simple single qubit phase rotation operation done after the transfer, we will neglect the effects of this shift in the following discussion.

Let us focus now on our specific system, the IPA. If we consider as a starting point a chain of similar QDs regularly spaced, and approximate the electron and hole wave-functions as Gaussian, we can estimate the Stark shift of the excitonic level of QD<sub>*i*</sub> in respect to the central, unperturbed, QD<sub>*np*</sub> produced by the application of the fields  $\{\mathcal{F}\}$  to satisfy Eq. (7) (see Fig. 2). This is given by

$$|E_i| = -\hbar\omega_{ex,i} \frac{1 + \frac{m_e\omega_{ex,i}}{m_h\omega_{hx,i}}}{1 + \frac{m_e\omega_{ex,i}^2}{m_h\omega_{hx,i}^2}} \ln \frac{J_i}{J_{max}}, \quad (18)$$

where  $J_{max} = \max\{J_i\}$  is the value of the coupling between QD<sub>*np*</sub> and its neighbors. The ratio  $J_i/J_{max}$  can be calculated from Eq. (7). For a given semiconductor, Eq. (18) depends on the ratio  $\omega_{ex,i}/\omega_{hx,i}$ , but for the relatively short IPAs we are considering, we see that, even when  $\omega_{ex,i}/\omega_{hx,i} \approx 3$  and  $\hbar\omega_{ex,i} = 20 \div 40$  meV,  $|E_i| > 1$ meV. When we consider the approximate sequence  $\{E_i\}$  as given by Eq. (18) and let the system evolve according to the Hamiltonian in Eq. (14), our simulations show that the excitonic transfer from the first to the last QD may be achieved, but depending on the parameters chosen. In Fig. 4 we compare the case of  $N=5$  (upper panel) and  $N=7$  for the same structural parameters (see figure caption) and  $|\psi(0)\rangle = |10\dots 0\rangle$ . Even when the transfer is achieved ( $N=5$ ), the periodic pattern becomes more complex and other excitonic states of the system are populated during the transfer itself (e.g. the probability of occupying state  $|00100\rangle$  is shown). For  $N=7$ , over the same interval of time, no relevant transfer across the chain is achieved, while the exciton remains mainly localized in QD<sub>1</sub>.

We can think of improving this result for relatively short IPA by requiring careful tuning of at least part of the distances  $R_{ij}$  between QDs and/or of other QDs parameters during the growth process, in order to obtain as a starting point a sequence of  $J_i$  which matches more closely the requirement of Eq. (7). This implies the application of *smaller static electric fields* and consequently smaller Stark shifts. The energy shifts will now be in general randomly distributed, depending on how well the single coupling  $J_{i,i+1}$  satisfies Eq. (7).

We have tested the robustness of this scenario by calculating the fidelity of the transfer across a QD chain in which the sequence  $\{E_i\}$  is produced randomly, with the constraint  $E_i \leq \delta E$ . The fidelity of the transfer for each set  $\{E_i\}$  is calculated according to Ref. 13 as

$$\langle F \rangle_{Bl} = \frac{|f_N| \cos \gamma}{3} + \frac{|f_N|^2}{6} + \frac{1}{2}, \quad (19)$$

with  $f_N = \langle 0\dots 1 | \exp(-iHt) | 1\dots 0 \rangle$ ,  $H$  given by Eq. (14)

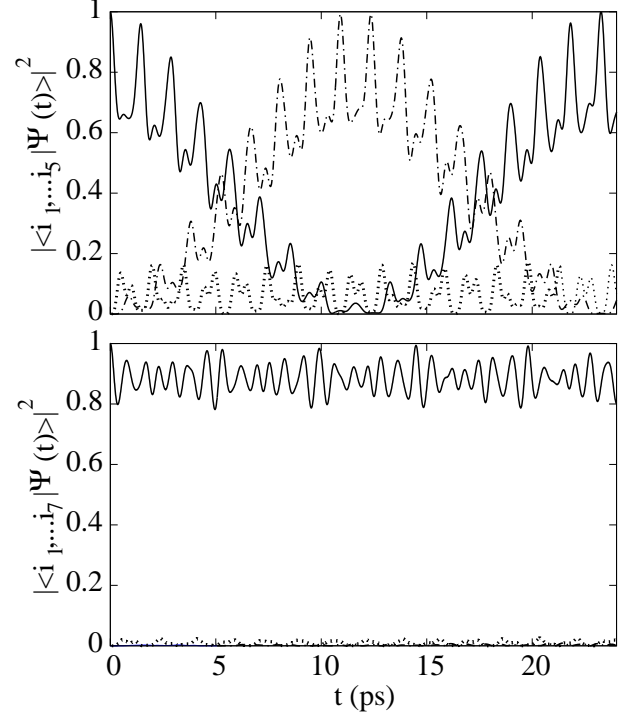


FIG. 4: Upper panel:  $|\langle 10000 | \psi(t) \rangle|^2$  (solid line),  $|\langle 00001 | \psi(t) \rangle|^2$  (dashed-dot line) and  $|\langle 00100 | \psi(t) \rangle|^2$  (dotted line) vs time, for  $J_{max} = 1$  meV,  $\hbar\omega_{ex,i} = 20$  meV and  $\omega_{ex,i}/\omega_{hx,i} = 3$  and GaAs parameters. Lower panel:  $|\langle 1000000 | \psi(t) \rangle|^2$  (solid line),  $|\langle 0000001 | \psi(t) \rangle|^2$  (dashed-dot line) and  $|\langle 0001000 | \psi(t) \rangle|^2$  (dotted line) vs time. Same parameters as upper panel.

and  $\gamma = \arg\{f_N\}$ . In the following we will set  $\cos \gamma = 1$  since we can always correct the phase shift after the transfer has occurred, as mentioned before. Notice that the fidelity in Eq. (19) includes the averaging of the initial state of QD<sub>1</sub> over the whole Bloch sphere<sup>13</sup>. The obtained result will be then averaged (when appropriate) over different random configurations  $\{E_i\}$  ( $\langle F \rangle_{Bl,cf}$ ). In this respect, when  $\delta E \gtrsim J_{max}$  it is important to perform this average over some thousand configurations, in order to obtain reliable results.

Results for IPAs with  $N=5$  and  $N=7$  are plotted in Fig. 5.  $\langle F \rangle_{Bl,cf}$  is plotted in respect to the value of  $J_{max}$ , for two different values of  $\delta E$ . The behavior for the two values is similar, the relevant parameter being the ratio  $\delta E/J_{max}$ . In particular, when  $\delta E \approx J_{max}$ , the fidelity is still greater than 90%, but it decreases drastically for increasing  $\delta E/J_{max}$ . The variation with the chain length is instead not substantial, though shorter chains perform better. Notice that in Ref. 15 the *opposite* trend is predicted, i.e. longer chains more robust than shorter ones. This is due to the fact that in their simulations they use different constraints: they vary  $N$  for fixed time transfer  $t_{1pk}$ , i.e. for fixed  $J$ . In other words the maximum value for the coupling between nearby spins is not fixed, and  $J_{max}$  is let increasing with the number of spins  $N$ .



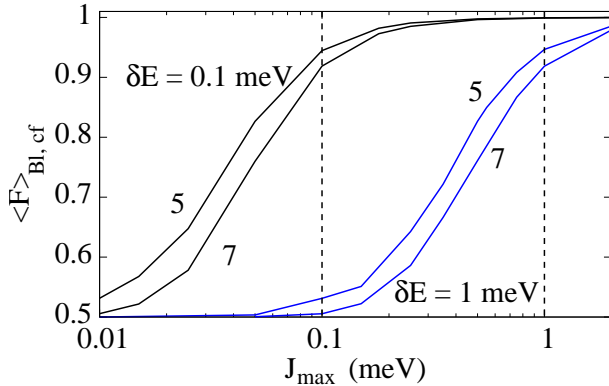


FIG. 5: Average fidelity  $\langle F \rangle_{Bl,cf}$  vs  $J_{max}$ , for  $\delta E = 0.1$  meV and  $\delta E = 1$  meV and chain length of 5 and 7 QDs, as labeled. The vertical dashed lines indicates the values for which  $J_{max} = \delta E$ .

When  $\delta E \gtrsim J_{max}$ , the fidelity of the transfer  $\langle F \rangle_{Bl}$  from first to last QD largely varies according to the specific set  $\{E_i\}$ . In addition the presence of  $\{E_i \neq 0\}$  modifies the time at which  $\langle F \rangle_{Bl}$  is maximum (the same occurs for the second method we shall consider, see inset of Fig. 8). In this respect a possible way to improve the fidelity would be to initially measure the optimal transfer time for the specific set  $\{E_i\}$  corresponding to the sample and then tune the time for the transfer operation accordingly. For IPAs the main contribution to  $\{E_i\}$  is given by growth and/or applied static electric fields, so that measuring the optimal transfer time for the specific hardware piece might recover a significant part of the fidelity. Nowadays tests on single electronic components are done routinely to check their specifications; we foresee that analogous testing procedures will be needed for the various hardware components of a quantum computer.

### E. Implementation by global dynamics using a QD chain: second method (flat coupling)

We have stressed in Sec. III A that the main advantage of using global dynamics should be to simplify the implementation of the computation. For implementing the MC method with IPAs, careful tuning of the QD properties is required both in the growth phase and a posteriori, with the risk that large values of  $E_i$  may result, affecting the fidelity. In order to simplify the implementation and overcome some possible sources of error, we will consider in this section the global dynamics of a spin chain, when all couplings between nearby spins are the same, i.e.  $J_k = J_i$ , and  $E_k = E_i$  for every  $i, k$ . We shall refer to this as “flat coupling” (FC) scheme. As underlined in Sec. II these requirements should be easier to match, at least considering implementations which use IPAs as hardware, since mastering these QD properties is already on the agenda of many experimental groups<sup>10,11</sup>.

We want to address the questions (i) if transfer of a quantum state across the chain by exploiting global dynamics is still

possible and with which degree of accuracy and (ii) how the results are affected by imperfections.

We consider again relatively short spin chains, with  $N = 1, \dots, 9$ , and simulate the evolution of the system according to the Hamiltonian Eq. (14). A similar problem have been analyzed in Ref. 13, but under different constraints and mainly considering the limit of long spin chains, so that properties of the relatively short chains which are relevant to the present proposal have not been discussed.

The inset of Fig. 6 shows the time evolution of a  $N=5$  chain with  $E_k = 0$ ,  $k = 1, N$  and  $J_{max} = 1$  meV. The upper panel presents the fidelity  $\langle F \rangle_{Bl}$  in respect to time; the lower panel shows the real (solid line) and the imaginary (dashed-dot line) components of the projection  $\langle 00001 | \Psi(t) \rangle$  in respect to time, with initial conditions  $|\Psi(0)\rangle = |10000\rangle$ . As can be seen, the time evolution *as a whole* presents a periodic behavior (within the numerical error), centered on the peak labeled with ‘C’. The period is proportional to  $1/J_{max}$ . Within this period many *high-fidelity resonances* are present, some of which correspond to a fidelity  $\langle F \rangle_{Bl} \sim 1$  (e.g.  $\langle F \rangle_{Bl}^A = 0.981$ ,  $\langle F \rangle_{Bl}^B = 0.996$  and  $\langle F \rangle_{Bl}^C = 1.00$ ). The behavior just discussed represents a typical pattern for all the spin-chains here analyzed. In particular, for  $N \leq 9$ , the very first resonance (labeled ‘A’ in the inset of Fig. 6) corresponds always to a fidelity  $\langle F \rangle_{Bl} > 94\%$  (Fig. 7, main panel). In general chains with an odd number of QDs  $N$  have an overall period shorter than the corresponding  $(N-1)$  QD chains. Interestingly the phase of the projection  $\langle 00001 | \Psi(t) \rangle$  follows for FC the same dependence on  $N$  as for MC, i.e. it is given by  $(-i)^{N-1}$ .

In the inset of Fig. 7, the time  $t_A$  at which the resonance ‘A’ occurs, is shown in respect to  $N$ . Both  $t_A$  and the corresponding fidelity  $\langle F \rangle_{Bl}^A$  present a *weak* linear dependence with the length of the chain  $N$ , with  $t_A$  though still below 2 ps for  $N=9$  (inset of Fig. 7). We stress that for the applications we are interested in, we need a finite, relatively small number of QDs, so these results are very encouraging.

In all cases analyzed, at least one of the resonances following peak ‘A’ corresponds to an even higher fidelity (e.g. B and C in Fig. 6, for  $N=5$ ). The possibility of accessing these stronger resonances as a mean of a better information transfer along the chain, will depend on the values of  $J_{max}$ , and of the typical decoherence times of the system, since, as already mentioned, the times corresponding to the different resonances scale as  $1/J_{max}$ .

We shall now analyze how the different resonances are influenced by imperfections. As for MC, we have considered sets  $\{E_i\}$  with  $E_i$ ’s randomly distributed and  $E_i \leq \delta E$ <sup>19</sup>. An average over an appropriate number of such configurations is taken to calculate the fidelity  $\langle F \rangle_{Bl,cf}$ . We present the results in Fig. 6, where the average fidelities  $\langle F \rangle_{Bl,cf}^K$ ,  $K = A, B, C$ , calculated at the times  $t_A, t_B$  and  $t_C$  at which the resonances occur, respectively, are plotted against  $\delta E$ . Our results show that the resonances B and C are less ‘robust’ in respect to the first resonance (A), i.e. they tolerate a lesser amount of imperfections in the flat distribution of the energies  $E_k$ . In fact for very small  $\delta E/J_{max}$ ,  $\langle F \rangle_{Bl,cf}^{B,C} \approx 1$ , while  $\langle F \rangle_{Bl,cf}^A = 0.98$ .  $\langle F \rangle_{Bl,cf}^{B,C}$  though decrease rapidly already

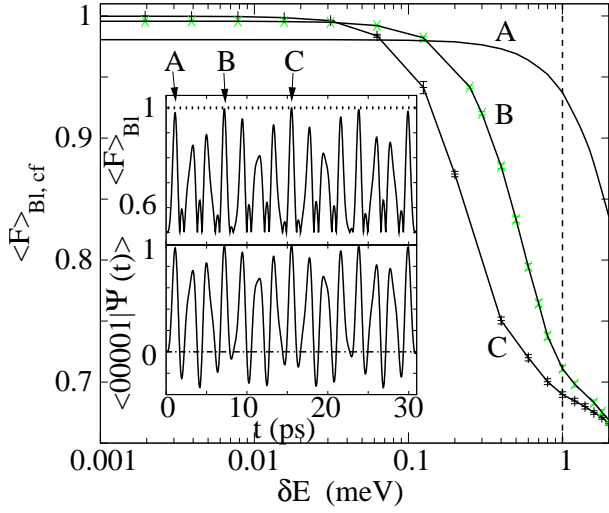


FIG. 6:  $\langle F \rangle_{Bl,cf}$  vs  $\delta E$  for three different resonances (labeled A,B and C), for  $N=5$  and  $J_{max} = 1$  meV. The dashed vertical line corresponds to the value of  $J_{max}$ . Inset: upper panel:  $\langle F \rangle_{Bl}$  as a function of time for  $\delta E = 0$ ,  $N=5$  and  $J_{max} = 1$  meV. Lower panel: real (solid line) and imaginary (dashed-dot line) part of  $\langle 00001 | \Psi(t) \rangle$  for  $|\Psi(0)\rangle = |10000\rangle$  and same parameters as upper panel.

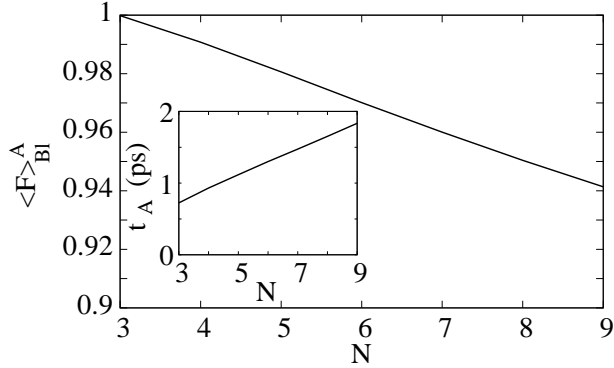


FIG. 7:  $\langle F \rangle_{Bl}^A$  vs  $N$ . Inset:  $t_A$  vs  $N$ . Parameters as inset of Fig. 6.

for  $\delta E/J_{max} \sim 0.1$ , while  $\langle F \rangle_{Bl,cf}^A$  remains basically unperturbed. For  $\delta E/J_{max} = 1$ ,  $\langle F \rangle_{Bl,cf}^{B,C}$  drop to about 0.7, while  $\langle F \rangle_{Bl,cf}^A \sim 0.94$ , still a very significant fidelity.

### F. Comparison between modulated and flat coupling

We shall now compare MC and FC schemes. In Fig. 8 we compare  $\langle F \rangle_{Bl,cf}^A$  (dashed-dot line), with the average fidelity  $\langle F \rangle_{Bl,cf}$  calculated at  $t_{1pk}$  (see Eq. (8)) with  $J_i$ 's given by Eq. (7) (solid line). They are plotted in respect to  $\delta E$ , which is varied up to 2 meV, for  $N=5$  and  $J_{max} = 1$  meV. We notice that for  $\delta E/J_{max} \approx 1.3$ , the fidelity of MC method becomes smaller, confirming that, if  $\delta E \gtrsim J_{max}$  is to be expected (e.g.

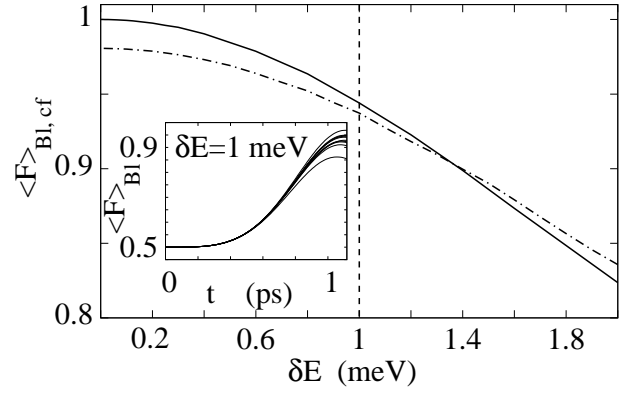


FIG. 8:  $\langle F \rangle_{Bl,cf}$  vs  $\delta E$  for MC scheme at  $t_{1pk}$  (solid line) and FC scheme at  $t_A$  (dashed-dot line).  $N=5$ ,  $J_{max} = 1$  meV. Inset:  $\langle F \rangle_{Bl}$  vs time for FC scheme and same parameter as main panel. The x-axis upper limit corresponds to  $t_A$ .

when using IPAs as hardware), it is convenient to opt for the simpler FC scheme. The inset of Fig. 8 presents  $\langle F \rangle_{Bl}(t)$  for FC in respect to time, for  $t \leq t_A$  and  $\delta E = 1$  meV. Each curve corresponds to a different random set  $\{E_i\}$ . The plot shows that  $\langle F \rangle_{Bl}^A$  is spread over a large interval which increases with increasing  $\delta E$  (not shown). Two things should be noticed, the first is that the fidelity corresponding to a specific  $\{E_k\}$  configuration can be (clearly) greater than the average fidelity  $\langle F \rangle_{Bl,cf}$ , the second that the maximum the fidelity for the transfer may occur at times different from  $t_A$ . Similar conclusions are reached when analyzing  $\langle F \rangle_{Bl}(t)$  in the MC scheme. These considerations imply that (i) operatively it will be important to carefully measure the sample characteristics in order to optimize the transfer time, and/or, as possible alternative, (ii) specific sets  $\{E_i\}$  could be designed to optimize the fidelity.

FC scheme can be seen as representing a very bad implementation of the MC scheme, in which every trace of the sequence Eq. (7) has been washed out. In this respect the occurrence of the very strong first resonance 'A' – resonance which coincides, time and strength, with the first transfer of the MC scheme when  $N \leq 3$  – suggests that, for relatively short chains, the MC scheme is very robust in respect to imperfections in the  $J_i$ 's sequence Eq. (7). This robustness decreases with  $N$ , as the strength of  $\langle F \rangle_{Bl}^A$  does (see Fig. 7)<sup>20</sup>. This interpretation also helps to understand why (i) the same phase dependence on  $N$  is observed in the FC and in the MC scheme for the projection  $\langle 00001 | \Psi(t) \rangle$  and (ii)  $t_A$  has a linear dependence on  $N$  similar to  $t_{1pk}$  (compare Fig. 3, lower panel, and inset of Fig. 7).

Our results suggest, for simplicity of implementation and especially if it is possible to have access to the resonances corresponding to the highest fidelities (B and C in Fig. 6) the FC as the best scheme, at least when using IPAs as hardware.



#### IV. SUMMARY AND CONCLUSIONS

We have proposed a potential implementation for a quantum computer where both the computation and the communication between far away qubits utilize exclusively quantum dot arrays. We have discussed how the different characteristics of in-plane and stacked arrays of QDs can be exploited to this purpose, the first as quantum buses and the second as quantum registers. The structure we propose is scalable and avoids the use of microcavities.

In the second part of the paper we have focused on the properties of the global dynamics of 'relatively short' spin chains, such chains been the most relevant in respect to the physical problem at hand. By mapping ground state excitons into (pseudo) spins, this dynamics can be used as a way to implement long distance communication between far away QDs connected by an in-plane array of QDs. We have discussed and compared two different potential schemes, the first based on the coupling between nearest-neighbor spins modulated along the chain<sup>12</sup>, the second based on a flat, uniform coupling. In particular, in the case of flat coupling, we have shown that the system presents a behavior overall periodic in time, containing a series of resonances corresponding to a fidelity of the state transfer across the chain very close to 100%. The very first of these resonances corresponds always to a high fi-

delity, *larger than 94%* for  $N \leq 9$ . This fidelity presents a linear dependence on the spin chain length  $N$ , but such a dependence is relatively weak. According to the system physical characteristics (maximum value of the nearest-neighbor coupling and decoherence times) one or all of these resonances will be accessible experimentally and exploitable as a mechanism for transferring information. The effects of imperfections on these resonances has also been analyzed, showing that the very first one is very robust.

It is clearly possible to design many more schemes to implement information transfer along in-plane QD chains – schemes either based on the global dynamics of the chain or on nearest-neighbor two-qubit gating. A systematic analysis of all possible schemes goes beyond the scope (and the possibilities) of this paper. We hope that the two potential implementations here discussed represent a good starting point for a stimulating discussion on the all-QD-based hardware structure we have proposed.

#### Acknowledgments

We are grateful to M. Feng, N. Datta, M. Christandl, A. Bychkov, T.P. Spiller, and B.W. Lovett for stimulating and fruitful discussions.

---

\* Electronic address: ida500@york.ac.uk

<sup>1</sup> Pierre M. Petroff, Axel Lorke, and Atac Imamoglu, *Physics Today* **54**, issue 5, 46 (2001).

<sup>2</sup> E. Biolatti, I. D'Amico, P. Zanardi and F. Rossi, *Phys. Rev. B* **65**, 075306 (2002).

<sup>3</sup> S. De Rinaldis, I. D'Amico, E. Biolatti, R. Rinaldi, R. Cingolani, and F. Rossi, *Phys. Rev. B* **65**, 081309 (2002).

<sup>4</sup> A. Nazir, B.W. Lovett, S.D. Barret, T.P. Spiller and G.A.D. Briggs, *Phys. Rev. Lett.* **93**, 150502 (2004); A. Nazir, B.W. Lovett, and G.A.D. Briggs, *Phys. Rev. A* **70**, 052301 (2004)

<sup>5</sup> M. Feng, I. D'Amico, P. Zanardi and F. Rossi, *Phys. Rev. A* **67**, 014306 (2003).

<sup>6</sup> M. Feng, I. D'Amico, P. Zanardi and F. Rossi, *Europhys. Lett.* **66**, 14 (2004).

<sup>7</sup> E. Pazy, E. Biolatti, T. Calarco, I. D'Amico, P. Zanardi, F. Rossi, P. Zoller, *Europhys. Lett.* **62**, 175 (2003).

<sup>8</sup> M.S. Sherwin, A. Imamoglu, and T. Montroy, *Phys. Rev. A* **60**, 3508 (1999)

<sup>9</sup> S. De Rinaldis, I. D'Amico, and F. Rossi, *Phys. Rev. B Phys. Rev. B* **69**, 235316 (2004).

<sup>10</sup> A. Moritz, R. Wirth, A. Hangleiter, A. Kurtenbach, and K. Eberl, *Appl. Phys. Lett.*, **69**, 212 (1996); Y K Su, S J Chang, L W Ji, C S Chang, L W Wu, W C Lai, T H Fang and K T Lam, *Semicond. Sci. Technol.* **19** No 3, 389 (2004); P.R. Edwards, R.W. Martin, I.M. Watson, C. Liu, R.A. Taylor, J.H. Rice, J.H. Na, J.W. Robinson and J.D. Smith, *Appl. Phys. Lett.*, **85**, 4281 (2004). Gao, M. Buda, H. H. Tan, C. Jagadish, *Electrochem. Solid-State Lett.* **8**, 57 (2005)

<sup>11</sup> G. Medeiros-Ribeiro, R. L. Maltez, A. A. Bernussi, D. Ugarte,

and W. de Carvalho, Jr., *Journal of Appl. Phys.* **89**, Issue 11, 6548 (2001); W. Ye, S. Hanson, M. Reason, X. Weng, and R.S. Goldman, *J. Vac. Sci. Technol. B* **23**, 1736 (2005); X. Weng, W. Ye, S.J. Clarke, R.S. Goldman, V. Rotberg, A. Daniel, and R. Clarke, *J. Appl. Phys.* **97**, 064301 (2005); Z. M. Wang, K. Holmes, Yu. I. Mazur, and G. J. Salamo, *Appl. Phys. Lett.* **84**, Issue 11, 1931 (2004).

<sup>12</sup> M. Christandl, N. Datta, T. C. Dorlas, A. Ekert, A. Kay and A.J. Landahl, *Phys. Rev. A* **71**, 032312 (2005)

<sup>13</sup> S. Bose, *Phys. Rev. Lett.* **91**, 207901 (2003)

<sup>14</sup> A. Woicik, T. Luczak, P. Kurzynsky, A. Grudka, T. Gdala and M. Bednarska, [quant-ph/0505097](https://arxiv.org/abs/quant-ph/0505097); L.F. Santos [quant-ph/0505072](https://arxiv.org/abs/quant-ph/0505072).

<sup>15</sup> G. De Chiara, D. Rossini, S. Montangero and R. Fazio, [quant-ph/0502148](https://arxiv.org/abs/quant-ph/0502148)

<sup>16</sup> R.S. Knox and H. Van Amerongen, *J. Phys. Chem. B* **2002**, 5289 (2002).

<sup>17</sup> S.A. Crooker, J.A. Hollingsworth, S. Tretiak, and V.I. Klimov, *Phys. Rev. Lett.*, **89**, 186802 (2002).

<sup>18</sup> B.W. Lovett, J.H. Reina, A. Nazir, B. Kothari and G.A.D. Briggs, *Phys. Lett. A*, **315**, 136 (2003).

<sup>19</sup> By applying external electric fields, imperfections on the coupling constants may be corrected and partially transformed into imperfections on the  $\{E_i\}$  set (as seen in the first part of the previous section), so for our purposes it is sufficient to study the effects of imperfections over the energy set.

<sup>20</sup> This conclusion is different from the one in Ref. 15 for the same reasons as for the effect of imperfections over the set  $\{E_i\}$ ,